

Ballistic Optimization of the Star Grain Configuration

Wm. Ted Brooks*

Hercules Incorporated, McGregor, Tex.

Ballistic design analysis of the star grain configuration involves parametric evaluation of the six dimensionless independent geometric variables that define the star. Because of the large, virtually limitless number of combinations of these variables that will satisfy requirements for volumetric loading and web fraction, a parametric approach is necessary if one is to insure that the final design is the optimal one based on performance. The analysis applied in this paper identifies, for a given volumetric loading fraction, the most neutral-burning star with given web fraction, symmetry number, and two small radii. The related computer program was used to generate data for evaluating various other optimization criteria for star designs and to establish some universal limits of the capability of the star in terms of neutrality and sliver.

Nomenclature

A_g	= total cross-sectional area of grain
A_s	= cross-sectional area of sliver
d	= half of minimum distance between star points (Fig. 1)
L/D	= length-to-diameter ratio
MEOP	= maximum expected operating pressure (limit on maximum pressure)
N	= star symmetry number, number of starpoints
P	= burning perimeter
P_{\max}	= maximum burning perimeter
\bar{P}_w	= average burning perimeter over web
\bar{P}_{wt}	= average burning perimeter over total web through sliver
R	= grain outside radius
R_f	= dimensionless fillet radius ($R_f = r_f/R$)
R_2	= dimensionless cusp radius ($R_2 = r_2/R$)
r	= bore radius, radius of circle tangent to starpoints (Fig. 1)
r_f	= fillet radius
r_2	= cusp radius
V_t	= volumetric loading fraction
w	= web thickness
w_f	= web fraction ($w_f = w/R$)
w_j	= web-burned distance to the end of zone 2 (Fig. 1); defined also as Y .
w_t	= total web through sliver (Fig. 1)
w_x	= variable web burned
Γ	= ratio of maximum to average burning perimeter (P_{\max}/\bar{P}_w)
Γ_{\min}	= minimum value of Γ achievable with a given V_t in a family of stars (fixed N , w_f , R_f , and R_2)
η	= star angle (Fig. 1)
λ	= ratio of initial perimeter to grain circumference ($r_f = r_2 = 0$)
ξ	= star angle (Fig. 1)
σ	= sliver fraction
μ	= ratio of minimum to initial perimeter ($r_f = r_2 = 0$)

Introduction

THE star grain configuration is applicable to a relatively wide range of web fractions and volumetric loading fractions. It provides reasonably neutral burning characteristics in two dimensions without the need of end effects and slots; thus, minimum insulation for protection of the chamber wall is required. In view of these characteristics, the star grain design has been widely used in solid rocket applications.

The seven independent geometric variables (six dimensionless variables) that define the star make it a very analytic grain configuration with seemingly endless mathematical relationships of practical interest. This analytic potential has resulted in many published works on methods of star analysis over the past 35 years or more.¹ Among the ones most frequently cited are those by Avery, Beek, and Shafer,¹⁻³ Stone,⁴ and Vandekerckhove.⁵ These early methods are characterized by graphs from which relationships among volumetric loading, sliver, and perimeter-web neutrality can be evaluated. A more recent star analysis that relates structural and ballistic characteristics was reported by Messner.⁶

The method of analysis for star grains as applied herein is a computer method⁷ that provides design data similar to those cited above. However, the method of Ref. 7 differs from the earlier methods in three important aspects: 1) it treats all six independent dimensionless variables, whereas Shafer and Stone treated different sets of four variables, Vandekerckhove five variables analytically with limited treatment of the sixth variable, and Messner five variables; 2) it applies for the neutrality parameter the ratio of maximum-to-average perimeter, which is a more meaningful design parameter than the progressivity ratio used in other methods (progressivity ratio is an alternate option in the analysis); and 3) it treats the volumetric loading fraction as a constant rather than a variable as treated in other analyses, i.e., each output star design is a unique solution that satisfies a specified volumetric loading fraction and neutrality criterion.

The analytic format of Ref. 7 provides an automated method for evaluating relationships among neutrality, sliver, and web fraction for a given volumetric loading fraction and the effect on star performance of variables frequently omitted in star analyses. Application of the method thus provides criteria for optimizing dimensions of all six independent dimensionless variables of the star. It was used in this effort to generate parametric design data for evaluating various optimization criteria for star designs and to establish some universal limits of the capability of the star in terms of neutrality and sliver.

Method of Analysis

The prime objective of the solid-propellant grain designer is to provide the rocket motor with a propellant grain that will

Presented as Paper 80-1136 at the AIAA/SAE/ASME 16th Joint Propulsion Conference, Hartford, Conn., June 30-July 2, 1980; submitted Aug. 25, 1980; revision received Sept. 21, 1981. Copyright © 1981 by Michael B. Keehan. Published by the American Institute of Aeronautics and Astronautics with permission.

*Staff Engineer, Hercules Aerospace Division. Associate Fellow AIAA.

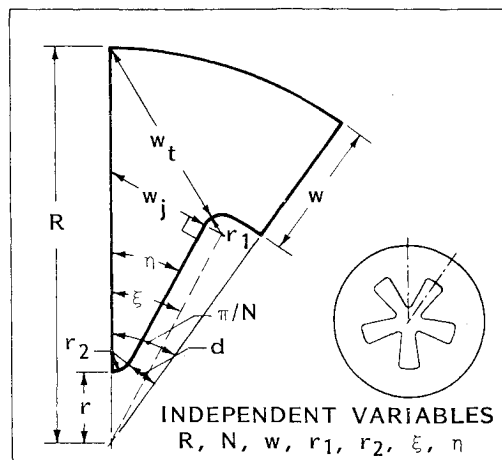


Fig. 1 Definition of the star grain configuration.

evolve combustion products consistent with the thrust-time schedule required for the mission. Geometric analysis is one part of this grain design process. There are many other considerations such as erosive burning and nozzle performance that are coupled analytically with the grain configuration through performance prediction to provide the final grain design that meets the rocket motor ballistic requirements. Nonetheless, geometric analysis is fundamental to grain design; and it is this aspect only that is considered here. Further, the star grain configuration is largely a two-dimensional grain design that is not necessarily dependent on three-dimensional end effects for burning neutrality. Therefore, only two-dimensional characteristics of the star configuration are treated here.

The method of Ref. 7 is summarized in this section. The ballistic star configuration is defined by seven independent geometric variables (Fig. 1). In dimensionless form, w , r_1 , and r_2 are given as a fraction of grain radius, in which case the number of variables is reduced to six. Four of these variables are commonly used: 1) web fraction $w_f (=w/R)$; 2) number of starpoints or symmetry number N ; 3) fillet radius $R_f (=r_1/R)$; and 4) cusp radius $R_2 (=r_2/R)$. The starpoint shape, however, has been defined in a variety of ways. In this analysis it is defined by two angles, ξ and η , variables of Refs. 1-3. The independent variables, then, are N , w_f , R_f , R_2 , ξ , and η . All stars with given N , w_f , R_f , and R_2 are referred to as a family of stars; and the remaining two variables ξ and η always function as dependent variables in a family of stars to satisfy a specified V_t and neutrality criterion.

Star grains are designed to satisfy several requirements, two notable ones being volumetric loading fraction and web fraction. Grain designs within a given family of stars that will satisfy these two criteria are virtually unlimited in number, as shown in Fig. 2 for a particular family of stars with $V_t = 0.80$. Each design is distinguished by a unique combination of ξ and η . They differ one from another in characteristics of burning neutrality and sliver content, the two major ballistic figures of merit for optimization. Therefore, ballistic analysis involves identification and evaluation of these candidates in terms of their burning neutrality and sliver content in search for the most optimal one. Many approaches to accomplish this have been reported (see citations in Ref. 7 in addition to references herein).

The three design parameters (volumetric loading, sliver, and a measure of burning neutrality) are of considerable importance in grain design analysis of a star. Frequently, the neutrality of a star has been evaluated in terms of the two ratios: λ , the ratio of initial perimeter to grain circumference; and μ , the minimum perimeter ratio.¹⁻³ The grain circumference in the ratio λ is almost but not exactly equal to the final perimeter. Jointly these two ratios give an approximate indication of the degree of neutrality.

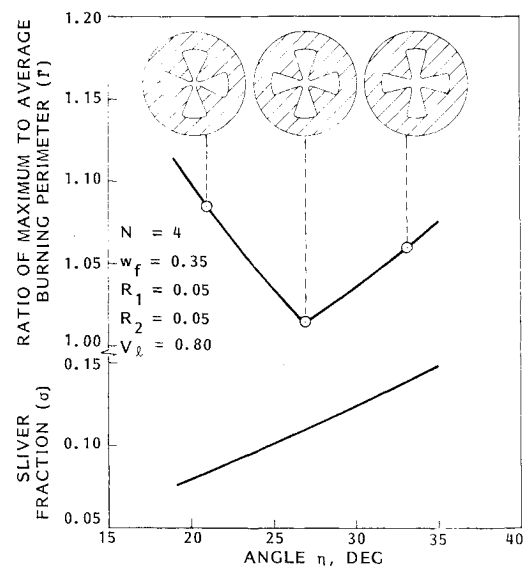


Fig. 2 Four-point star grain designs with 35% web fraction and 80% volumetric loading.

The most significant measure of neutrality (in two dimensions) of a given star is the ratio of maximum-to-average burning perimeter since this ratio indicates the ratio of maximum-to-average pressure. With this parameter the average pressure can be estimated from the maximum expected operating pressure (MEOP) (or MEOP from a given average pressure). Average pressure is a parameter in preliminary design effort that is vital to the process of determining a reasonably accurate preliminary volumetric loading requirement. Thus, the relative value of maximum burning perimeter is equally important. This analysis, therefore, centers around evaluation of the ratio of maximum-to-average burning perimeter (Fig. 2).

There are two average perimeters that are important in ballistic analysis of configured grains, with the significance of each depending on the optimization criterion: 1) the average perimeter over the web interval w [$\bar{P}_w = (A_g - A_s)/w$]; and 2) the average perimeter over the total web interval through the sliver w_t ($\bar{P}_{wt} = A_g/w_t$). These two criteria are described below.

1) Usually one considers neutrality in terms of the flatness of the thrust-time trace. This aspect of neutrality is important and, in fact, is an explicit requirement in some specifications. The perimeter ratio that relates directly to the flatness of the thrust-vs-time curve is maximum-to-average perimeter over web (P_{max}/\bar{P}_w). The notation Γ is used for this ratio. The star design in a given family of stars that satisfies a given V_t with minimum Γ (Γ_{min}) is referred to as the star having optimal neutrality.

2) More important in many instances is the ratio of maximum pressure and the average pressure that relates to delivered specific impulse. This ratio for star designs depends on sliver content as well as on the flatness of the pressure-time trace. Other parameters being equal, the motor that operates at an overall average pressure (e.g., average over action time) nearest the maximum pressure will deliver the greatest specific impulse (at sea level). Operating a motor at an average pressure near the maximum pressure is the underlying purpose for neutrality. The perimeter ratio that relates approximately to this pressure ratio is the ratio of maximum-to-average perimeter over total web through sliver (P_{max}/\bar{P}_{wt}).

The unique combination of ξ and η that produces Γ_{min} also produces the minimum ratio P_{max}/\bar{P}_{wt} . Consider the behavior of Γ_{min} when only web fraction varies. The parameter Γ_{min} itself will have a minimum value for some web fraction, as will the minimum value of P_{max}/\bar{P}_{wt} . These relationships are shown in Table 1 for an example in which $N=5$,

Table 1 Neutrality as a function of w_f for $v_l = 0.85$

w_f	Γ_{\min}	Min P_{\max}/\bar{P}_{wt}	σ	ξ , deg	η , deg
0.31	1.041	1.413	0.159	30.15	26.74
0.33	1.004 ^a	1.329	0.167	31.66	31.04
0.43	1.084	1.257 ^a	0.064	26.48	22.60
0.45	1.113	1.259	0.049	24.81	19.58

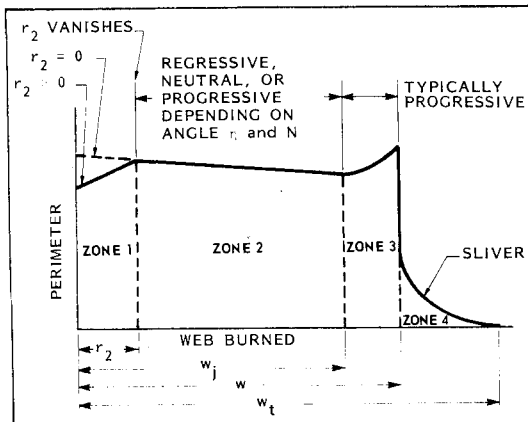
^aMinimum value with respect to web fraction.

Fig. 3 Burning characteristics of the star.

Table 2 Unique combinations of N and n for neutrality in zone 2

N	η , deg
3	24.55
4	28.22
5	31.13
6	33.53
7	35.56
8	37.31
9	38.84
10	40.20

$R_1 = R_2 = 0.05$, and $V_l = 0.85$. Thus, the optimal star design in the example based on the criterion of neutrality or flatness of the perimeter-vs-web curve would have $w_f = 0.33$ and a rather large sliver fraction of 0.167; whereas, the optimal star design based on impulse delivery at sea level would have $w_f = 0.43$ with larger Γ_{\min} but much less sliver than the design with minimum Γ_{\min} (see Ref. 7 for additional discussion).

It is noted that the analysis does, in fact, identify the unique star in a family of stars that has minimum Γ . However, this star design typically has large starpoints that may result in a small clearance between starpoints and a small bore radius (d and r , Fig. 1). The bore radius is a dependent variable but will always be greater than zero if $R_2 > 0$; and $d \geq 0$. Quantitative effects of R_2 on these dimensions are discussed subsequently. It should also be recognized that for $\Gamma_{\min} > 1$, a minimum point on the perimeter-web curve will occur when the web burned = w_j . Star designs with relatively large Γ_{\min} likewise will have relatively low minimum points. Consequently, even though optimum in terms of impulse delivery, the perimeter-web curve may have a minimum saddle point for relatively large Γ_{\min} that may be undesirable if only because of appearance.

Star Optimization

The computer program of Ref. 7 was used to generate parametric design data for evaluating several characteristics of the star, principally the tradeoffs between neutrality and sliver, relationship of symmetry number N to optimization, and effect of geometric limitations on ballistic optimization.

Characteristics of the Sharp-Pointed Star

Stars with $R_1 = R_2 = 0$ (the sharp-pointed star) generally are not practical. However, they are considered here as a point of reference, since 1) sliver is minimum when $R_1 = 0$, and 2) $R_2 = 0$ is a necessary condition for total neutrality of perimeter vs web.

The star has four distinct phases of burning (Fig. 3). It is always linear and progressive until the web burned equals R_2 (zone 1). In zone 1, $dP/dw_x = 2\pi$ regardless of star dimensions. Zone 2 is linear and is either neutral, progressive, or

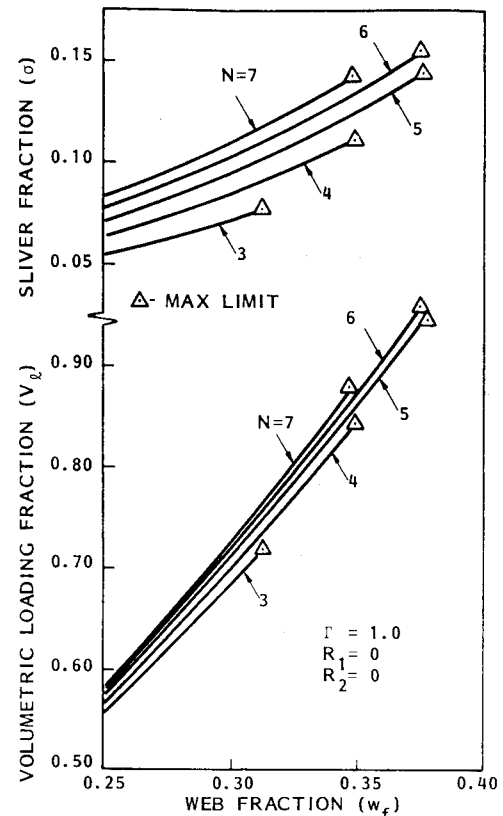


Fig. 4 Characteristics of the neutral burning sharp-pointed star.

regressive depending on N and η . For a given N , neutrality ($dP/dw_x = 0$) is achieved in zone 2 if, and only if, η has the unique value corresponding to N shown in Table 2.

Zone 3, when it exists, is usually progressive; and the sliver burning in zone 4 is always regressive. Therefore, total neutrality ($\Gamma_{\min} = 1$) over web is achieved only when zones 1 and 3 do not exist ($R_2 = 0$ and $w_j = w$) and η has the necessary value with respect to N .

In order for $w_j = w$, the following relation must exist

$$\xi = \sin^{-1} \left(\frac{w_f + R_1}{1 - w_f - R_1} \cos \eta \right) \quad (1)$$

Table 3 Limiting w_f for neutral sharp-pointed stars

N	Limiting w_f	η , deg	ξ , deg	V_ℓ	σ
3	0.314	24.55	24.55	$(< \pi/N)$	0.078
4	0.349	28.22	28.22	$(< \pi/N)$	0.112
5	0.377	31.13	31.13	$(< \pi/N)$	0.144
6	0.375	33.53	30.00	$(= \pi/N)$	0.154
7	0.348	35.56	25.71	$(= \pi/N)$	0.142

Table 4 Four-point stars with $V_\ell = 0.80$ having optimal neutrality ($R_1 = R_2 = 0.05$)

w_f	Γ_{\min}	σ	ξ , deg	η , deg
0.30	1.045	0.135	29.61	23.42
0.31	1.025	0.140	30.46	25.68
0.32	1.006	0.143	31.23	27.96
0.33	1.005	0.133	31.03	28.08
0.34	1.008	0.121	30.57	27.65
0.35	1.014	0.110	30.01	26.98
0.36	1.021	0.098	29.34	26.11
0.37	1.031	0.087	28.60	25.08
0.38	1.042	0.077	27.77	23.90
0.39	1.054	0.067	26.87	22.55
0.40	1.068	0.058	25.91	21.11
0.41	1.082	0.049	24.89	19.56
0.42	1.098	0.041	23.80	17.87
0.43	1.115	0.034	22.64	16.07
0.44	1.132	0.028	21.42	14.16
0.45	1.151	0.022	20.12	12.12

The radius $R_1 = 0$ in the case under consideration. For a neutral star with a given N and web fraction, the value of angle η is defined by N and the value of ξ is defined jointly by η and w_f [Eq. (1)]. Therefore, only one neutral star design exists for a given N and web fraction. Characteristics of these neutral stars for combinations of N and w_f are shown in Fig. 4. Volumetric loading, sliver, and cross-sectional loading without sliver increase with web fraction.

Neutral stars corresponding to the limiting web fraction for each N in Fig. 4 are shown in Table 3. An interesting point arises from these relationships. If V_ℓ were considered as a continuous function of N (N not limited to being an integer), volumetric loading would be a maximum of 100% at a point $5 < N < 6$, where ξ is first large enough to equal π/N . Specifically, at $N = 5.54$, $\xi = \eta = \pi/N = 32.48$ deg and $w_f = 0.389$, and the star has 100% volumetric loading with sliver of 16.2%. This condition, of course, does not exist.

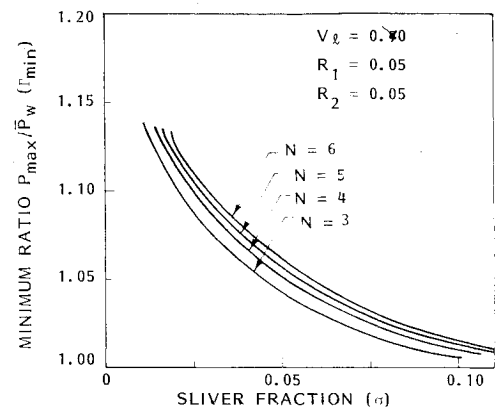
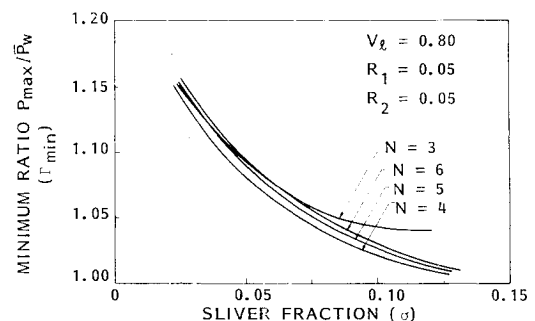
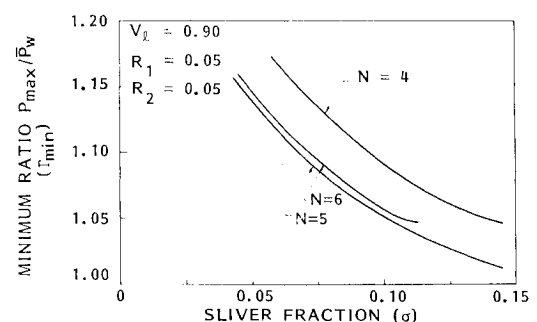
Some of the relationships in this section are discussed in more detail in Ref. 7.

Effect of N on Optimization

One of the major considerations in ballistic design analysis for star optimization is the tradeoff between sliver and neutrality. The designer normally has a requirement for volumetric loading that has been established in view of an attendant sliver fraction. These two requirements plus a third, a neutrality criterion, can be satisfied jointly by three of the star variables— w_f , ξ , and η . For the criteria $V_\ell = 0.80$ and $\sigma = 0.10$, for example (see Table 4 for $N = 4$), the most neutral star has $\Gamma_{\min} = 1.021$ and is defined by $w_f = 0.358$, $\xi = 29.5$ deg, and $\eta = 26.3$ deg. Similarly, for three-point stars $\Gamma_{\min} = 1.043$ and for five-point stars $\Gamma_{\min} = 1.026$. Therefore, the most neutral star that satisfies the given volumetric loading and sliver criteria is the four-point star.

To evaluate the effect of N on optimization, data were generated (in the format of Table 4) for volumetric loading fractions in the range 0.7-0.9 for three-to-five-point stars. Parametric plots of these results showing the variation of Γ_{\min} with sliver fraction are shown in Figs. 5-7.

The symmetry number N for stars with smallest Γ_{\min} depends on volumetric loading. At $V_\ell = 0.70$, the three-point

Fig. 5 Neutrality vs sliver for stars with $V_\ell = 0.70$.Fig. 6 Neutrality vs sliver for stars with $V_\ell = 0.80$.Fig. 7 Neutrality vs sliver for stars with $V_\ell = 0.90$.

star has the smallest Γ_{\min} for any value of sliver in the range plotted; for $V_\ell = 0.80$, the four-point star is optimum; and for $V_\ell = 0.90$, the five-point star is optimum. A crossplot of these curves for 10% sliver (Fig. 8) shows the volumetric loading fractions at which the optimal symmetry number changes.

Effect of Volumetric Loading on Neutrality and Sliver

When the solid motor design requires a highly loaded, internal-burning, configured grain, the star configuration applies. The impact of attendant sliver content on the design depends on the specific ballistic requirements; however, in virtually all instances the sliver fraction will have a bearing on the required volumetric loading. At one extreme is an impulse

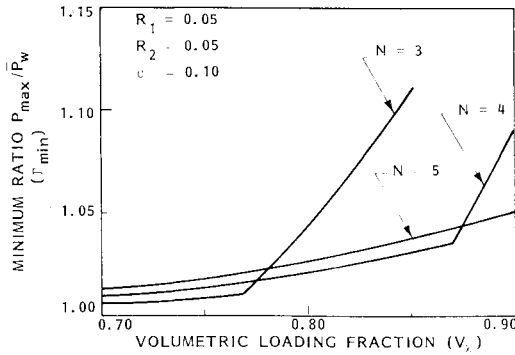


Fig. 8 Neutrality vs volumetric loading fraction for $\sigma = 0.10$.

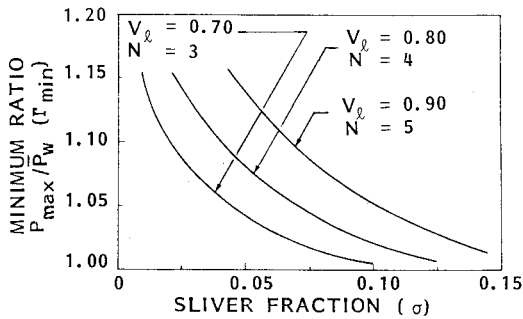


Fig. 9 Effect of volumetric loading on sliver and neutrality.

requirement only for burn time impulse, in which case the sliver would not contribute to meeting performance requirements. At the other extreme is a requirement for deliverable total impulse (zero to zero), in which case the sliver would contribute to motor performance but at a lower motor efficiency because of the reduced average thrust coefficient. In any event, the sliver fraction must be reconciled.

If burning neutrality is not important, high volumetric loading fractions can be achieved with small sliver fractions by increasing the web fraction. The limit, of course, is a design with web fraction sufficiently large to obtain the volumetric loading requirement without starpoints, in which case the design would have no sliver. In this case the volumetric loading is defined simply by

$$V_l = w_f(2 - w_f) \quad (2)$$

which is the volumetric loading fraction of a circular-ported grain, applicable in general to $L/D < 2$.

Star designs with high volumetric loading that are optimum with respect to burning neutrality will have very pronounced starpoints and, therefore, significant sliver. The tendency is an increase in sliver fraction with volumetric loading for the optimal star. The quantitative effects of volumetric loading on sliver and neutrality are shown in Fig. 9. Volumetric loading fraction is given for the symmetry number N that was shown previously to be most optimum for the particular V_l , i.e., $N=3$ for $V_l=0.7$, $N=4$ for $V_l=0.8$, and $N=5$ for $V_l=0.9$. For a given sliver fraction Γ_{\min} increases significantly with increased volumetric loading fraction.

Effect of R_1 and R_2 on Design Optimization

From a ballistic standpoint, the grain designer would prefer relatively small, if not zero, R_1 and R_2 . Zero values, of course, are not practical because of grain process and structural requirements. Effects R_1 and R_2 have on ballistic and geometric characteristics are discussed below.

Table 5 Effect of R_1 on σ and Γ_{\min}

R_1	η , deg	ξ , deg	σ	Γ_{\min}
0	27.87	25.86	0.090	1.007
0.05	26.98	30.01	0.110	1.014
0.10	25.44	34.61	0.133	1.026
0.15	22.94	39.83	0.162	1.044

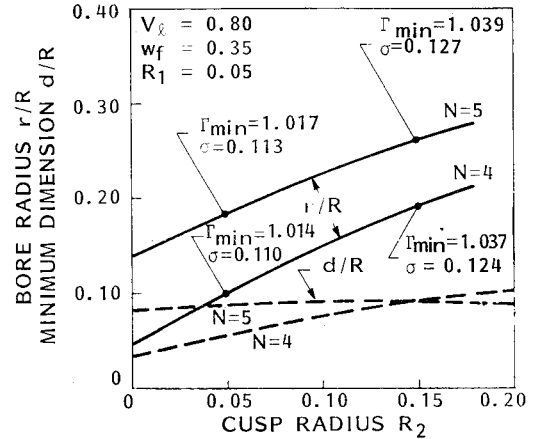


Fig. 10 Effect of cusp radius R_2 on port dimensions r and d for stars having optimal neutrality.

Fillet Radius R_1

Because angle ξ locates the vertex of R_1 , variation in R_1 with fixed N , w_f , R_2 , and V_l tends to effect a like variation in ξ . Sliver fraction in a family of stars is largely a function of ξ in which larger values of ξ will produce larger sliver fractions; therefore, the magnitude of R_1 in a family of stars has a bearing on the magnitude of sliver fraction. This effect of R_1 on sliver fraction, also on Γ_{\min} , is illustrated in the example shown in Table 5, a tabulation of four-point star grain designs with optimal neutrality for $V_l=0.80$ having $w_f=0.35$ and $R_2=0.05$. In this example, σ is almost proportional to ξ and R_1 . The effects of R_1 on σ and Γ_{\min} , therefore, are quite significant.

Cusp Radius R_2

A totally neutral perimeter-vs-web trace cannot be achieved with $R_2 > 0$, as shown previously. For a grain design having optimal neutrality that satisfies a given volumetric loading fraction, an increase in R_2 without compensating changes in other dimensions decreases the volumetric loading fraction. With the larger R_2 , as with R_1 , the grain design for the same volumetric loading fraction, web fraction, and N will optimize at a greater angle ξ with greater values of Γ_{\min} and sliver. In general, however, neutrality and sliver are not as sensitive to changes in R_2 as to changes in R_1 .

The most notable consequences of a small cusp radius R_2 are proportionately small port dimensions near the center of the grain, namely the bore radius r and the minimum distance $2d$ between star tips when $\eta < \pi/N$ (see Fig. 1). The starpoint of the star with optimal neutrality is necessarily very pronounced and the resulting clearance between star tips for these optimal designs may be small. A relatively small dimension here could be a concern in mandrel fabrication and perhaps in two-dimensional erosive burning considerations.

Relationships among R_2 , Γ_{\min} , sliver fraction, and the two port dimensions r and d are illustrated in Fig. 10 for the stars indicated. For the four-point star with $R_2=0.05$ (used in previous graphs) in a 10 in. diameter motor, for example, the bore diameter would be only 1.0 in. and the minimum distance between star tips ($2d$) 0.6 in. These values could be increased for the four-point star to 1.9 and 0.9 in., respectively, by increasing R_2 to 0.15. Over this interval of R_2 , both

sliver and Γ_{\min} increase significantly. However, these larger port dimensions could be achieved with the five-point star at $R_2 = 0.05$ with much less compromise in ballistic optimization (Γ_{\min} and σ values). Therefore, with minimum values of Γ_{\min} and σ as the only criteria, the four-point star in this case would be optimum for $V_t = 0.80$. Imposing also the criteria that d and r be maximum, the five-point star would be optimum. For $N = 6$ on this graph, $\eta > \pi/N$ and the dimension d is not defined, in which case the minimum distance between starpoints occurs near the base of the point rather than at the tip.

Conclusions

The first level of optimization of a star design for a given volumetric loading fraction is the evaluation of the effects of web fraction and N on the neutrality parameter Γ_{\min} and sliver fraction, assuming moderately small R_1 and R_2 . In this evaluation with a given N , Γ_{\min} increases and sliver fraction decreases as the web fraction increases, which requires ballistic and perhaps structural evaluation of the tradeoffs among these parameters. The value of N for optimal neutrality depends on the volumetric loading fraction, in which larger values of N apply to larger volumetric loading fractions. In general, Γ_{\min} for a given sliver fraction increases with V_t .

In consideration of R_1 and R_2 , ballistic optimization favors small values while structural requirements and characteristics of port geometry favor larger values. Consideration of port dimensions r and d as well as Γ_{\min} and σ may have a bearing on the optimal value of symmetry number N . Thus, tradeoffs among these parameters should be evaluated.

Therefore, each of the six independent variables of the star configuration— N , w_f , R_1 , R_2 , ξ , and η —has a bearing on specific aspects of star optimization. Each star that is optimum in one respect frequently has another characteristic that is much less optimum. Because of these attributes of the star, compromises will result and only an analysis of a suitable range of candidate stars satisfying the volumetric loading requirement will insure an overall optimal design. The method of analysis of Ref. 7 is a comprehensive analytical tool for conducting this analysis.

References

- ¹Avery, W.H. and Beek, J. Jr., "Propellant Charge Design of Solid Fuel Rockets," Office of Scientific Research and Development, Rept. 5809, June 1946.
- ²Piasecki, L. and Robillard, G., "Generalized Design Equations for an Internal-Burning Star-Configuration Solid-Propellant Charge and Method of Calculating Pressure-Time and Thrust-Time Relationships," JPL Memo 20-135, Sept. 1956.
- ³Bartley, C.E. and Mills, M.M., "Solid Propellant Rockets," *Jet Propulsion Engines*, Sec. H., edited by E.O. Lancaster, Princeton University Press, Princeton, N.J., 1959.
- ⁴Stone, M.W., "A Practical Mathematical Approach to Grain Design," *Jet Propulsion*, Vol. 28, April 1958, pp. 236-244 (comment in Vol. 28, Nov. 1958, pp. 766-768).
- ⁵Barrere, M., Jaumotte, A., Fraeijs de Veubeke, B., and Vandenkerckhove, J., *Rocket Propulsion*, Sec. 6.2, Elsevier Publishing Co., New York, 1960.
- ⁶Messner, A.M., "Final Report Integrated Structural and Ballistic Design Curves for Star-Perforated Propellant Grains," AFRPL-TR-70-106, Oct. 1970.
- ⁷Brooks, W.T., "An Exact Practical Analysis of the Ballistic Star Configuration," *Proceedings of 1979 JANNAF Propulsion Meeting*, CPIA Pub. 300, Vol. II, May 1979, pp. 343-361.

From the AIAA Progress in Astronautics and Aeronautics Series . . .

REMOTE SENSING OF EARTH FROM SPACE: ROLE OF "SMART SENSORS"—v. 67

Edited by Roger A. Breckenridge, NASA Langley Research Center

The technology of remote sensing of Earth from orbiting spacecraft has advanced rapidly from the time two decades ago when the first Earth satellites returned simple radio transmissions and simple photographic information to Earth receivers. The advance has been largely the result of greatly improved detection sensitivity, signal discrimination, and response time of the sensors, as well as the introduction of new and diverse sensors for different physical and chemical functions. But the systems for such remote sensing have until now remained essentially unaltered: raw signals are radioed to ground receivers where the electrical quantities are recorded, converted, zero-adjusted, computed, and tabulated by specially designed electronic apparatus and large main-frame computers. The recent emergence of efficient detector arrays, microprocessors, integrated electronics, and specialized computer circuitry has sparked a revolution in sensor system technology, the so-called smart sensor. By incorporating many or all of the processing functions within the sensor device itself, a smart sensor can, with greater versatility, extract much more useful information from the received physical signals than a simple sensor, and it can handle a much larger volume of data. Smart sensor systems are expected to find application for remote data collection not only in spacecraft but in terrestrial systems as well, in order to circumvent the cumbersome methods associated with limited on-site sensing.

505 pp., 6 × 9, illus., \$22.00 Mem., \$42.50 List

TO ORDER WRITE: Publications Dept., AIAA, 1290 Avenue of the Americas, New York, N. Y. 10019